Available online at www.sciencedirect.com
ScienceDirect
Tetrahedron
Tetrahedron 63 (2007) 7386–7396

Composites of *N*,*N*′-bis-(pyridyl) urea-dicarboxylic acid as new hydrogelators—a crystal engineering approach

N. N. Adarsh, D. Krishna Kumar and Parthasarathi Dastidar*

Analytical Science Discipline, Central Salt and Marine Chemicals Research Institute (CSIR Laboratory), G.B. Marg, Bhavnagar 364 002, Gujarat, India

Received 9 September 2006; revised 8 December 2006; accepted 1 February 2007
Available online 7 February 2007

Abstract—Sixteen composites of a hydrogelator *N*,*N*′-bis(4-pyridyl) urea **1** and a nongelator *N*,*N*′-bis(3-pyridyl) urea **2** with a series of dicarboxylic acids having various backbones have been prepared and characterized. Seven such composites—three from the composites of **1** and four from the composites of **2**—turned out to be good to moderate gelling agents for pure water. Single crystal X-ray structures of three such gelators and four nongelators indicate that microporosity in the crystalline solid state structure may be one of the important criteria for hydrogelation.

1. Introduction

Low molecular mass organic gelators (LMOGs)[1] are interesting and useful organic compounds capable of gelling different organic and aqueous fluids. Organogelators are those capable of gelling organic fluids whereas hydrogelators are able to harden aqueous fluids including pure water. It is believed, based on various physico-chemical measurements such as optical microscopy, electron microscopy (e.g., SEM, TEM), atomic force microscopy (AFM), X-ray diffraction, dynamic light scattering, small angle neutron scattering, etc., that the gelator molecules form some kind of 3D fibrous aggregates via spontaneous self-assembly process involving various intermolecular interactions such as hydrogen bonding, π-stacking, van der Waals, etc. and the bulk solvents are immobilized within such 3D network causing gelation.

Hydrogelators are an important class of gelling agents having various potential applications.[2] Hydrogelators are generally made from high molecular weight natural[3] and synthetic[4] polymers. However, non-polymeric self-assembly driven hydrogels derived from LMOGs have attracted attention because of the amenability to tune the gel properties by changing the chemical functionality, preparation conditions such as pH and temperature, and composition of the aqueous solution. In contrast to their organogelator counterpart, non-polymeric hydro-gelling agents based on LMOGs are indeed limited. This is due to the fact that LMOGs are often insoluble or poorly soluble in water as well as displaying high crystallinity in water. Moreover, structural requirement for a molecule to become a hydrogelator is critical; it is believed that careful balance between hydrophobic interactions and hydrogen bonding in water or aqueous solution is essential to achieve the required 3D elastic networks of small gelator molecules within which the solvent is immobilized.

The key to design new LMOGs lies in the molecular level understanding as to how the gelator molecules self-assemble to form the 3D intertwined network of fibers within which the solvent is immobilized to form a gel. However, it is virtually impossible to get this insight because single crystal X-ray diffraction methods cannot be applied to such nanofibers; only indirect powder diffraction methods may be applied in suitable cases.[5] However, recording good quality X-ray powder diffraction (XRPD) data of the gel fibers in their native form generally suffers from the scattering contribution of the solvent molecules and the less crystalline nature of the gel fiber and therefore, in most cases, attempts to record XRPD of gel fibers proved frustrating. On the other hand, correlating the single crystal structure of a molecule in its thermodynamically more stable crystalline state compared to its gel state with its gelling/nongelling behavior is more practical. We have shown with many single crystal structures that an 1D hydrogen bonded network is important for organo-gelation[6] and subsequently, we have identified supramolecular synthons[7] that predictably form 1D hydrogen bonded networks and induce gelation in organogel systems.[8] However, such structure–property correlations virtually do not exist in hydrogelator systems.

We have recently reported the crystal structures and the hydrogelation properties of various hydrogen bond functionalized pyridyl compounds;[9] these results tend to suggest that

* Corresponding author. Tel.: +91 278 2567760; fax: +91 278 2567562; e-mail addresses: parthod123@rediffmail.com; dastidar@csmcri.org

0040–4020/$ - see front matter © 2007 Elsevier Ltd. All rights reserved.
doi:10.1016/j.tet.2007.02.005

a microporous architecture in the crystalline solid state of a compound may be an important criterion for its hydrogelation behavior.[10]

More recently, we have crystallographically revealed the interactions of a hydrogelator molecule namely *N*,*N*′-bis-(4-pyridyl) urea **1** with its gelling solvents—water and ethylene glycol; interestingly, its isomers namely *N*,*N*′-bis(3-pyridyl) urea **2** and *N*,*N*′-bis(2-pyridyl) urea **3** were not capable of gelling aqueous solvents.[11] In an attempt to tailor the structure and property of **1** (hydrogelator) and **2** (nongelator), we realized that it was worthwhile to study various dicarboxylic acid salts/adducts of **1** and **2**, which are expected to generate new supramolecular structures and optimistically, novel properties of these salts/adducts. In the case of the dicarboxylate salt of the urea derivative, the dianionic acid moiety is expected to form a urea-carboxylate synthon (Scheme 1), which upon further self-assembly through hydrogen bonding is likely to generate a microporous architecture that appears to be an important criterion for hydrogelation; whereas, in the case of the adduct, the assembly of acid–urea could yield a 1D infinite hydrogen bonded network via the pyridine-carboxylic acid synthon (Scheme 1) the primary structure of which would depend on the topologies of the interacting species.

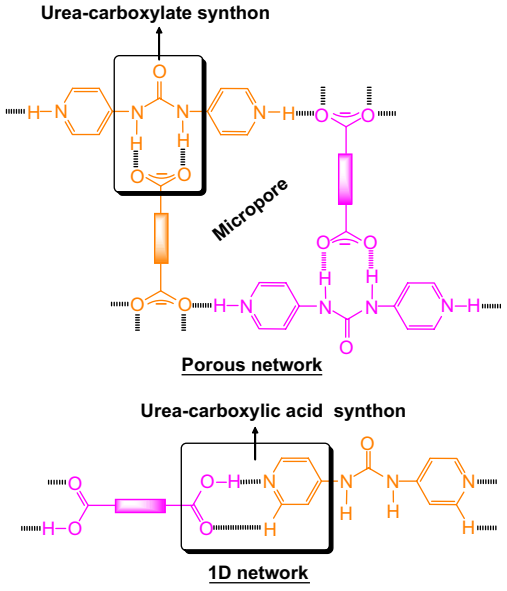

Scheme 1.

In this article, we present the preparation and hydrogelation properties of salts/adducts of **1** and **2** derived from a series of dicarboxylic acids having various backbones (Scheme 2). X-ray single crystal structures of seven such salts/adducts are discussed in the context of their structures and properties (gelation).

2. Results and discussions

2.1. Preparation and characterization of the dicarboxylic acid salts/adducts of 1 and 2

Preparation of the salts/adducts of **1** and **2** was carried out by reacting the corresponding acid and urea derivative in an

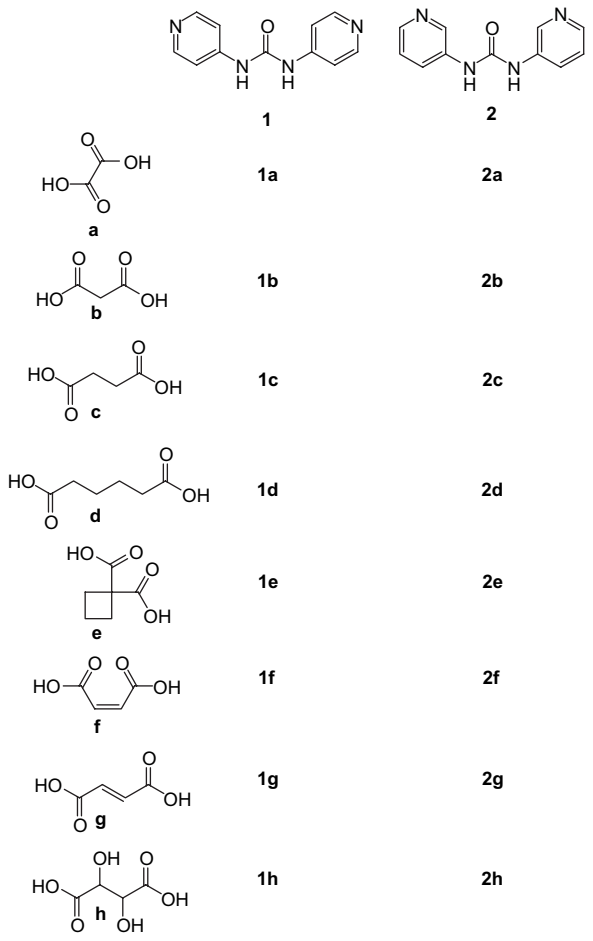

Scheme 2.

equimolar ratio (see Section 4). FTIR analyses of the solids indicate that complete proton transfer or salt formation took place in all the cases except in **1**·malonic acid (**1b**), **2**·succinic acid (**2c**), and **2**·adipic acid (**2d**). The absence of any peak in the region 1650–1550 cm^{-1} (for COO^-) and the presence of 1689 cm^{-1} (for COOH) in **2c** clearly indicate that it is a complex rather than a salt. On the other hand, bands at 1622 and 1604 cm^{-1} in **1b** and **2d**, respectively, are assigned to the COO^- functionality indicating salt formation. However, COOH bands at 1665 and 1701 cm^{-1} in these two compounds indicate partial salt formation. ^1H NMR data indicate the formation of 1:2 (acid/urea) salts in **1b**, **1c**, and **2g** although the starting molar ratio of the reacting species was 1:1 (acid/urea); whereas the rest of the adducts/salts were of 1:1 (acid/urea) stoichiometry.

2.2. Gelation studies

In a typical experiment, the compound was dissolved in water/aqueous solvents. The solution was then heated and cooled to room temperature. After cooling, the container (usually a test tube) was inverted to check the deformity of the material. If no deformation was observed, it was termed a gel. Table 1 gives the hydrogelation data of the compounds prepared herein.

Seven compounds namely **1**·succinic acid (**1c**), **1**·adipic acid (**1d**), **1**·maleic acid (**1f**), **2**·oxalic acid (**2a**), **2**·succinic

Table 1. Gelation data

Salts/adducts	M.G.C/wt % (w/v)	T_{gel}/°C (at M.G.C.)
1c	1.38	98
1d	1.4	72
1f	1.5	82
2a	2.12	78
2c	2.62	66
2f	1.17	80
2h	1.66	64

acid (**2c**), **2**·maleic acid (**2f**), and **2**·L-tartaric acid (**2h**) were found be good hydrogelators of pure water with low minimum gelator concentrations of ~1–3 wt % (w/v). The gels are opaque, stable over a period of several weeks, and display thermoreversible properties. All the composite gelators are organic salts rather than hydrogen bonded complexes except **2c**, which is a complex as revealed by FTIR analyses (see above). It is interesting to note that the parent ureas **1** and **2** are gelator and nongelator, respectively.[11] Thus, by forming composites with various dicarboxylic acids, the gelation properties of the parent ureas are altered. The fact that only seven out of sixteen composite of ureas studied herein show gelation properties indicates that perhaps the extent of protonation at ring N atoms of the corresponding ureas and the nature of the counter-anions indeed play an important role in tailoring the gelation properties.

2.3. Morphology of gel fibers

To examine the morphological structures of the gel fibers, scanning electron microscopy was performed on various xerogels. Figure 1 depicts the morphological characteristics of the xerogels of the gelators reported herein. While 1D slender fibers were observed in the xerogels of **1c** and **1d**, a mixture of plate shaped and 1D slender fibers was prevalent in the xerogel of **1f**. On the other hand, the gelators derived from **2** showed different types of morphologies. Thus, the xerogel of **2a** displayed a complicated 3D network of fibers of tape morphology and those of **2c** and **2f** showed intertwined network of 1D fibers and bundles of fibers. On the other hand, flexible rod type fibers are observed in the xerogel of **2h**. In all the cases, the fibers are tens of micrometers long and the thickness varied from submicron to tens of micrometers.

2.4. X-ray crystallography

Although the crystal structure of the gel fibers in its native gel state and that of the gelator in its neat crystalline state need not necessarily be identical, useful correlation between the crystal structure in neat crystalline state of a molecule and its gelling/nongelling behavior could be made as discussed above. Thus, it was important to study the crystal structures of as many composites studied herein as possible. X-ray quality single crystal structures of three hydrogelators namely **1c**, **1d**, and **2c** and four nongelators namely **1e**, **2d**, **2e**, and **2g** could be grown (see Section 4 and Table 2).

2.4.1. Single crystal structure of 1·succinic acid (1c). The hydrogelator **1c** belongs to the centrosymmetric triclinic space group $P\bar{1}$. The asymmetric unit includes two completely deprotonated succinic acid moieties, four monoprotonated urea derivatives, one solvate MeOH, 10 fully occupied solvate water molecules, and a partially occupied electron density peak around a center of symmetry, which was assigned as the O atom of a disordered water solvate. The C–O bond distances, which are in the range of 1.246(5)–1.271(5) Å, the absence of a parent acid COOH peak at 1694 cm^{-1}, and the presence of COO^- peak at 1627 cm^{-1} in FTIR clearly indicate complete salt formation. However, each acid donates its protons to pyridyl moieties of two independent urea derivatives **1** resulting in the formation of a 1:2 (acid/urea) salt rather than forming 1:1 salt as originally intended. Both the dicarboxylate moieties in the asymmetric unit display *gauche* conformation (dihedral angles 60.0° and 63.5°) and hold two monoprotonated urea derivatives displaying urea-carboxylate synthon [N···O=2.649(4)–2.933(4) Å; ∠N–H···O=165.2–173.5°] resulting in the formation of 'U' shaped ionic species; such ionic species are further self-assembled through N–H···N hydrogen bonding [N···N=2.656(4)–2.705(5) Å; ∠N–H···N=172.8–176.9°] involving protonated and non-protonated ends of the pyridyl groups of the adjacent ionic species thereby forming a 1D zigzag infinite chain. Such chains are further packed in a parallel fashion resulting in the formation of a microporous architecture (Fig. 2); the solvate water and MeOH molecules are located in such pores stabilized by various types of hydrogen bonding among themselves as well as with the carboxylate O atoms (Supplementary data).

2.4.2. Single crystal structure of 1·adipic acid (1d). The hydrogelator **1d** crystallizes in the centrosymmetric triclinic space group $P\bar{1}$. The asymmetric unit is comprised of one fully protonated pyridyl urea derivative **1**, one fully deprotonated adipic acid dianion, and three solvate water molecules. The C–O bond distances in the range of 1.255(5)–1.274(5) Å confirm complete proton transfer. Moreover, the absence of the parent COOH band at 1693 cm^{-1} and the presence of COO^- band at 1619 cm^{-1} further reinforce the salt nature of **1d**. In the crystal structure, the urea NH donor recognizes one end of the adipate dianion via urea-carboxylate synthon [N···O=2.749(4)–2.787(4) Å; ∠N–H···O=167.0–170.2°]. The other end of the adipate holds two neighboring protonated urea derivatives via N–H···O hydrogen bonding [N···O=2.564(4)–2.649(4) Å; ∠N–H···O=165.8–167.4°]. Such arrangements lead to the formation of a microporous 1D tape. The void spaces of the pores are occupied by a hydrogen bonded water tetramer [O···O=2.808(4)–2.828(5) Å; ∠O–H···O=161.2(3)–174.0(5)°] and a dimer [O···O=2.582(8)–2.611(8) Å] in an alternating fashion.

Within the respective pores, the water tetramer and the dimer are further hydrogen bonded with the respective carboxylate O atoms of the adipate dianion [O···O=2.778(5) Å; ∠O–H···O=160.0(3)° and O···O=2.702(4) Å; ∠O–H···O=157.0(6)°, respectively]. Due to their location around center of symmetry, the tetramer and the dimer display 1D staircase and zigzag network, respectively. The microporous tapes are further packed on top of each other down the *a*-axis creating infinite channels, which are occupied by the water staircase and zigzag network (Fig. 3).

2.4.3. Single crystal structure of 2·succinic acid (2c).[12] Hydrogelator **2c**, on the other hand, crystallizes in the centrosymmetric monoclinic *C*2/*c* space group. The asymmetric unit comprised of the hydrogen bonded complex of the

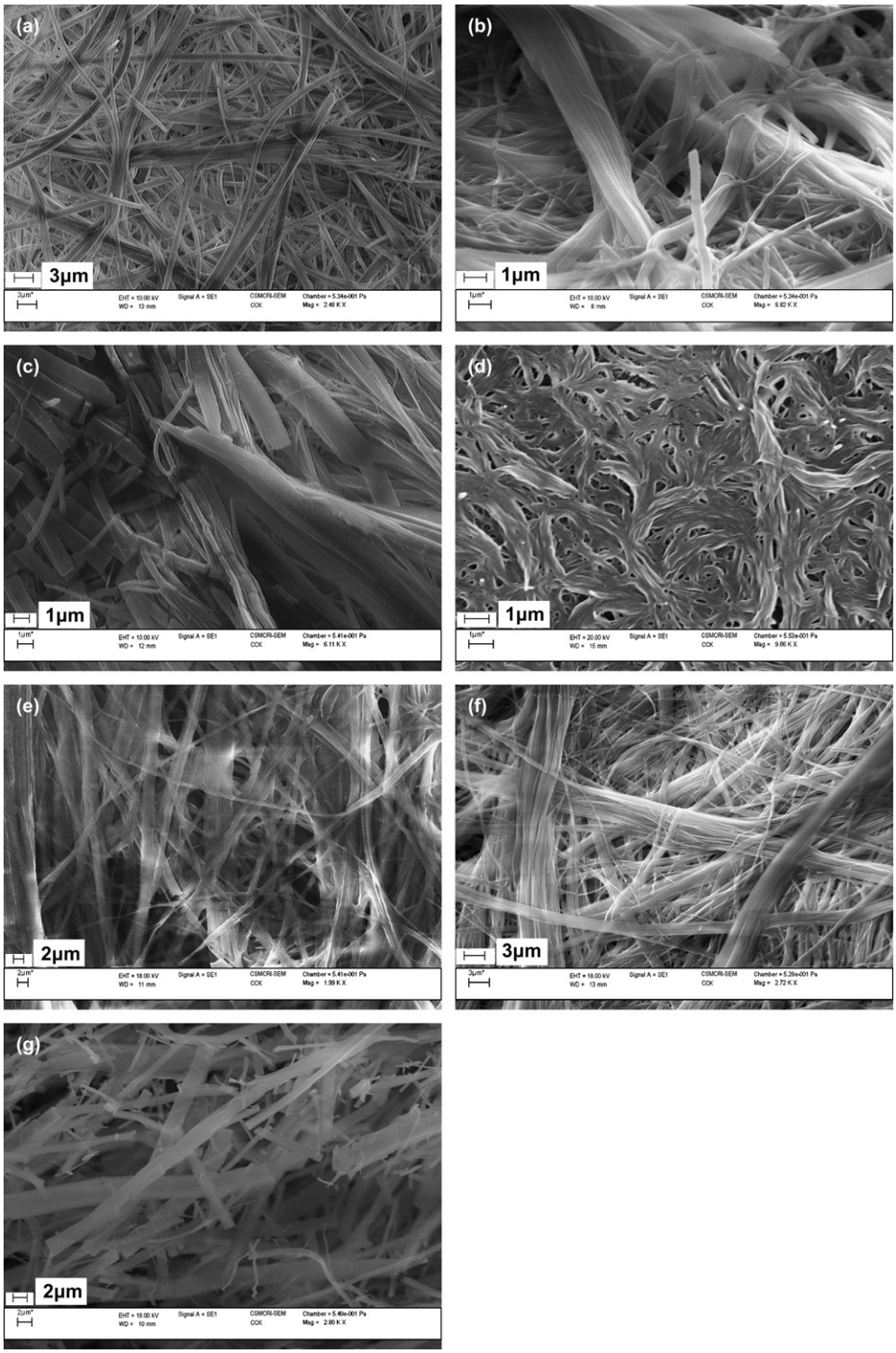

Figure 1. SEM micrographs of various xerogels of (a) **1c** (1.5 wt %); (b) **1d** (1.5 wt %); (c) **1f** (1.5 wt %); (d) **2a** (3.0 wt %); (e) **2c** (2.7 wt %); (f) **2f** (1.2 wt %); (g) **2h** (1.7 wt %).

pyridyl urea derivative **2** and succinic acid as revealed from the C–O bond distances, which are in the range of 1.196(2)–1.308(2) and 1.226(2)–1.283(2) Å in both the acid functionality of the succinic acid moiety. The absence of any FTIR band in the range of 1550–1650 cm^{-1} also confirms the complex rather than salt nature of **2c**. The urea derivative **2** adopts a *syn–anti* conformation. Each succinic acid holds two adjacent urea derivatives **2** via pyridine-carboxylic acid synthon [O···N=2.564(2)–2.647(2) Å; ∠O–H···N= 166.0(3)–175.0(3)° and C···O=3.216(3)–3.311(3) Å; ∠C–H···O=128.4–154.3(2)°] resulting in the formation of an 1D helical chain. Neighboring helical chains are further self-assembled by urea-carboxylate hydrogen bonding [N···O=2.777(2)–3.026(2) Å; ∠N–H···O=150.2(2)–164.5(2)°]

Table 2. Crystallographic parameters for **1c**, **1d**, **1e**, **2c**, **2d**, **2e**, and **2g**

Crystal data	**1c**	**1d**	**1e**	**2c**	**2d**	**2e**	**2g**
Empirical formula	$C_{53}H_{66}N_{16}O_{23.5}$	$C_{17}H_{26}N_4O_8$	$C_{17}H_{18}N_4O_5$	$C_{15}H_{16}N_4O_5$	$C_{28}H_{34}N_8O_8$	$C_{17}H_{18}N_4O_5$	$C_{13}H_{12}N_4O_3$
Formula weight	1303.30	413.41	358.35	332.32	610.63	358.35	272.27
Crystal size (mm^3)	0.35×0.22×0.07	0.32×0.18×0.06	0.46×0.32×0.16	0.32×0.22×0.07	0.31×0.24×0.10	0.33×0.18×0.09	0.32×0.18×0.08
Crystal system	Triclinic	Triclinic	Monoclinic	Monoclinic	Triclinic	Monoclinic	Monoclinic
Space group	*P*-1	*P*-1	$P2_1/c$	*C*2/*c*	*P*-1	$P2_1/c$	$P2_1/n$
a (Å)	9.2955(8)	4.6568(8)	7.5726(12)	38.107(10)	8.8184(8)	11.074(4)	7.289(1)
b (Å)	15.3113(14)	13.524(2)	19.745(3)	5.276(2)	11.3897(11)	8.070(3)	15.029(3)
c (Å)	22.1192(19)	16.979(3)	11.948(15)	16.454(4)	15.6818(15)	20.610(5)	11.673(2)
α (°)	84.159(2)	111.14(3)			106.901(2)		
β (°)	85.755(2)	95.697(3)	113.31(1)	109.31(4)	90.364(2)	118.02(2)	99.058(3)
γ (°)	85.901(2)	97.53(3)			108.941(2)		
Volume ($Å^3$)	3116.7(5)	976.3(3)	1640.7(4)	3122.1(1)	1416.6(2)	1626.0(9)	1262.7(4)
Z	2	2	4	8	2	4	4
D_{calcd} (g/cm^3)	1.389	1.406	1.451	1.414	1.432	1.464	1.432
F(000)	1368	438	752	1392	644	752	568
μ Mo Kα (mm^{-1})	0.111	0.113	0.109	0.108	0.107	0.110	0.105
Temperature (K)	298(2)	150(2)	298(2)	298(2)	100(2)	298(2)	298(2)
Range of *h*, *k*, *l*	−10/8, −16/16, −23/23	−5/4, −14/14, −18/17	−9/10, −26/23, −15/10	−49/47, −3/7, −19/21	−11/6, −13/14, −20/20	−14/14, −10/10, −20/27	−9/9, −14/19, −15/13
θ min/max	1.55/22.50	1.30/22.50	2.06/28.23	2.27/28.28	1.99/28.25	2.08/28.20	2.23/28.18
Reflections collected/unique/observed	12497/8043/5960	3885/2505/1892	9743/3809/2749	8544/3573/2425	8515/6252/5048	9267/3724/2963	7170/2844/2102
Data/restraints/parameters	8043/0/867	2505/0/270	3809/0/303	3573/0/236	6252/0/434	3724/0/236	2844/0/229
Goodness of fit on F^2	1.067	1.097	1.071	1.064	1.001	1.060	1.215
Final *R* indices [$I>2\sigma(I)$]	R_1=0.0636, wR_2=0.1774	R_1=0.0563, wR_2=0.1451	R_1=0.0613, wR_2=0.1323	R_1=0.0582, wR_2=0.1285	R_1=0.0466, wR_2=0.1323	R_1=0.0504, wR_2=0.1350	R_1=0.0736, wR_2=0.1844
R indices (all data)	R_1=0.0873, wR_2=0.2092	R_1=0.0790, wR_2=0.1759	R_1=0.0876, wR_2=0.1434	R_1=0.0901, wR_2=0.1421	R_1=0.0579, wR_2=0.1470	R_1=0.0623, wR_2=0.1469	R_1=0.1023, wR_2=0.1961

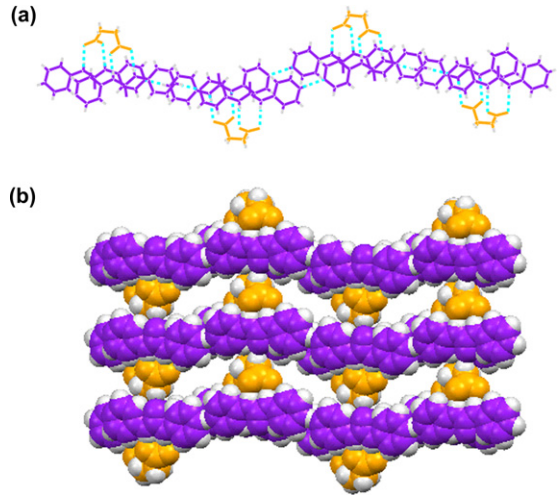

Figure 2. Illustration of crystal structure of **1c**: (a) zigzag 1D network of the ionic species; (b) microporous self-assembly of such 1D network; solvent molecules are not shown; acid and urea moieties are shown in orange and purple, respectively.

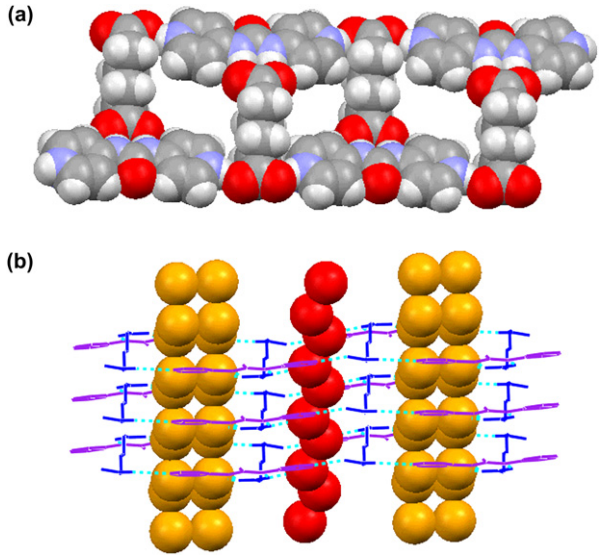

Figure 3. Crystal structure illustration of hydrogelator **1d**: (a) microporous ladder network displaying large pores; (b) side view of the ladder networks packed on top of each other displaying the tetramer (orange) and dimer (red) containing water clusters passing through the channels.

resulting in the formation of a 2D microporous network approximately along *b*–*c* plane (Fig. 4). The micropores, however, are filled by adjacent layers because of offset packing.

2.4.4. Single crystal structure of 1·cyclobutane-1,1-dicarboxylic acid (1e). Nongelator **1e** belongs to the centrosymmetric monoclinic space group $P2_1/c$ and the asymmetric unit contains one completely protonated **1** and 1,1-cyclobutane dicarboxylate moiety. The C–O bond distances, which are in the range of 1.224(2)–1.272(2) Å and the presence of FTIR band at 1632 cm^{-1} firmly indicate that complete proton transfer has taken place in **1e**. In the crystal structure, the cationic moiety holds two adjacent carboxylate moieties via N–H···O hydrogen bonding [N···O=2.540(2)–2.577(2) Å; ∠N–H···O=163.9–171.0(3)°] to result an 1D zigzag chain.

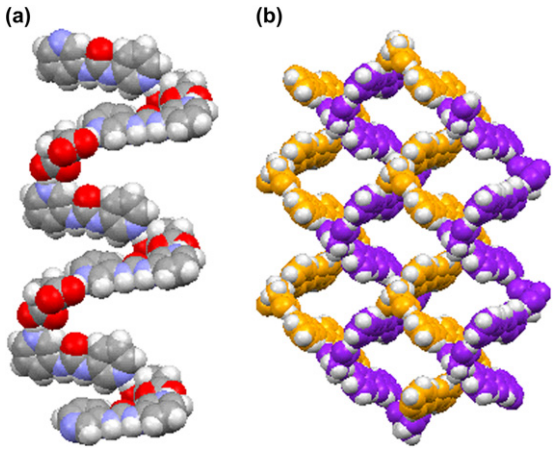

Figure 4. Illustration of crystal structure of hydrogelator **2c**: (a) helical 1D chain of ion pairs; (b) self-assembly of helical chains displaying microporous network.

Such chains are further self-assembled via N–H···O hydrogen bonding involving the urea functionality of the cation and the carboxylate moiety of the anion [N···O=2.707(2)–2.929(2) Å; ∠N–H···O=161.0(2)–168.0(2)°] resulting in the formation of a 2D hydrogen bonded microporous network propagating approximately parallel to the diagonal of the *a*–*c* plane. Offset packing of such planes effectively blocked the micropores in the crystal (Fig. 5).

2.4.5. Single crystal structure of 2·adipic acid (2d). Nongelator **2d** crystallizes in the centrosymmetric triclinic space group $P\bar{1}$. The asymmetric unit contains a monoprotonated urea derivative, monoanionic adipic acid moiety, a non-protonated urea derivative, and two solvate water molecules. The monoanionic nature of the adipic acid moiety is further supported by FTIR bands at 1701 cm^{-1} (COOH) and 1604 cm^{-1} (COO^-) and C–O distances [1.257(2)–1.263(2) Å for COO^- and 1.214(2)–1.326(2) Å for COOH]. In the crystal structure, the monoanionic adipic acid moiety holds two urea derivatives via N–H···O hydrogen bonding; while the carboxylate end of the adipic acid moiety interacts with the monoprotonated urea moiety involving carboxylate O atoms and urea N atoms [N···O=2.716(2)–2.865(2) Å; ∠N–H···O=174.9(2)–176.0(2)°], the carboxylic acid moiety forms hydrogen bonding with the non-protonated urea involving

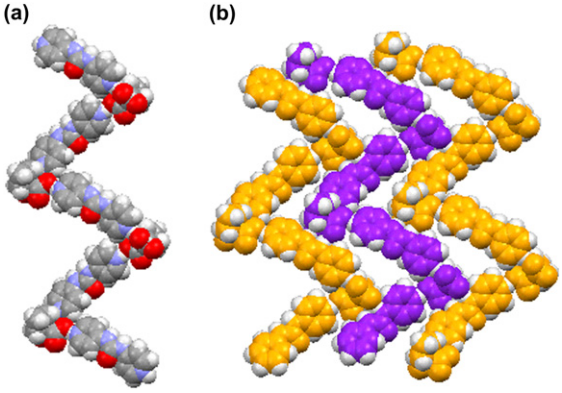

Figure 5. Crystal structure of nongelator **1e**: (a) zigzag 1D chain of ion pairs; (b) assembly of 1D chains.

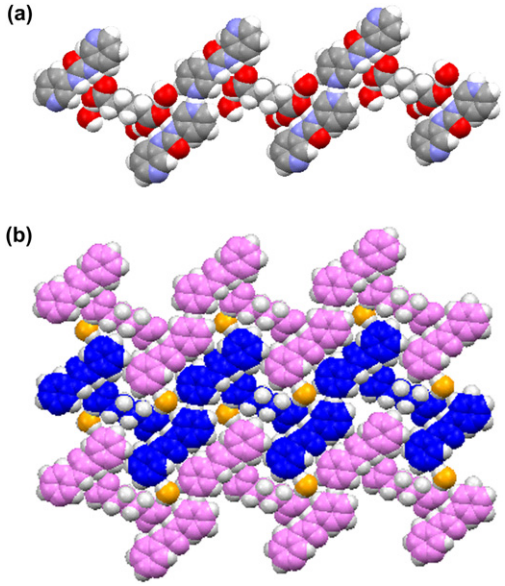

Figure 6. Crystal structure illustration of nongelator **2d**: (a) zigzag propagation of 'I' shaped ionic species; (b) further self-assembly of zigzag 1D chains mediated by water (orange) hydrogen bonding; interacting zigzag chains are shown in pink and blue in an alternating fashion.

carbonyl O atom of COOH group and N–H of urea moiety [N···O=2.910(2) Å; ∠N–H···O=167.2(2)°]. Such adducts of monoprotonated urea-hydrogen adipate–non-protonated urea further self-assemble through N–H···N hydrogen bonding with the neighboring adducts [N···N=2.670(2) Å; ∠N–H···N=178.6(2)°] resulting in an 1D zigzag polymeric chain. Such chains are further packed approximately perpendicular to the *a*–*b* plane mediated by hydrogen bonding with the solvate water molecules involving O–H···O, O–H···N, and N–H···O interactions [O···O=2.571(2)–2.770(2) Å; ∠O–H···O=167.0(3)–177.0(2)°; O···N=2.828(2)–2.899(2) Å; ∠O–H···N=175.0(2)–178.0(2)°; N···O=2.924(2) Å; ∠N–H···O=136.0(2)°] (Fig. 6).

2.4.6. Single crystal structure of 2·cyclobutane-1,1-dicarboxylic acid (2e). The nongelator **2e** is found to be crystallized in the centrosymmetric monoclinic space group $P2_1/c$. In the asymmetric unit, one 1,1-cyclobutane dicarboxylic acid moiety and one urea derivative are found. C–O bond distances of the acid moiety [1.235(2)–1.261(2) Å for COO^- and 1.202(2)–1.324(2) Å for COOH] and the presence of FTIR bands at 1591 cm^{-1} (COO^-) and 1697 cm^{-1} (COOH) clearly indicate partial salt formation. The 3-pyridyl urea derivative is found to be monoprotonated and displays *syn–anti* conformation. In the crystal structure, the COO^-···HOOC synthon is observed involving O–H···O hydrogen bonding [O···O=2.615(2) Å; ∠O–H···O=172.0°] resulting in the formation of an 1D zigzag infinite chain of acid moieties. Each acid moiety in the chain is further hydrogen bonded with the monoprotonated urea moiety displaying urea-carboxylate synthon involving N–H···O hydrogen bonding [N···O=2.815(2)–2.829(2) Å; ∠N–H···O=161.9–173.7°]. Such ion pair chains are further self-assembled through N–H···N hydrogen bonding [N···N=2.773(2) Å; ∠N–H···N=152.7°] arising from the protonated and non-protonated end of the urea moieties of the neighboring chains resulting in the formation of a 2D hydrogen bonded network propagating parallel to the *a*-axis. It can be seen that

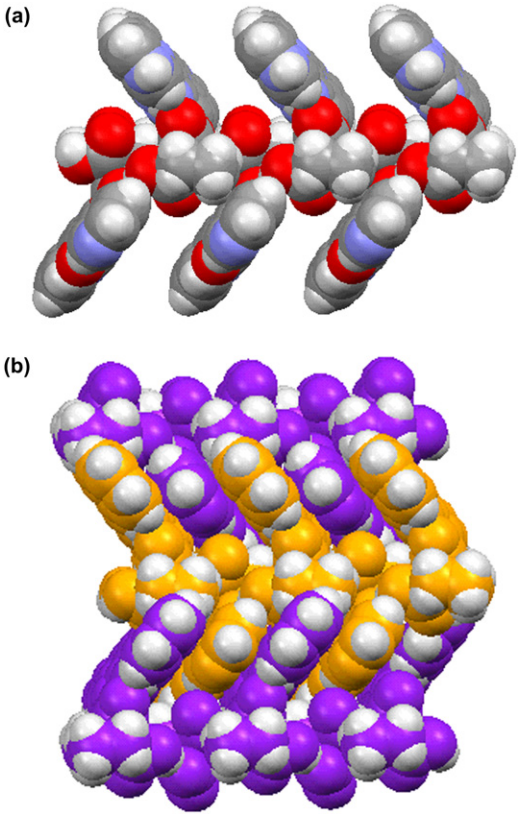

Figure 7. Crystal structure of **2e**: (a) double toothed zipper architecture; (b) self-assembly of the zippers via interdigitation of urea moieties; interacting zippers are shown in violet and orange in an alternating fashion.

due to the perpendicular orientation of the urea moieties in the 2D hydrogen bonded network, a double toothed zipper type of structure is formed. As a result, such 2D networks are further packed in a parallel fashion displaying excellent interdigitation of the urea moieties (Fig. 7).

2.4.7. Single crystal structure of 2·fumaric acid (2g). Nongelator **2g** crystallizes in the centrosymmetric monoclinic space group $P2_1/n$. Interestingly, the asymmetric unit contains half of the fumaric acid moiety and one monoprotonated urea. The other half of the acid moiety is generated by a 2-fold axis. As a result, one fully deprotonated fumaric acid moiety is present in the crystal structure, which is further hydrogen bonded to two monoprotonated pyridyl urea derivatives via urea-carboxylate synthon [N···O=2.692(3)–2.756(3) Å; ∠N–H···O=167.0(4)–171.0(3)°]. The complete salt formation in **2g** is also evident from the C–O bond distances of the acid moiety [1.236(4)–1.240(4) Å] as well as the presence of a FTIR band at 1633 cm^{-1} (COO^-). The 'I' shaped ionic species are further hydrogen bonded via N–H···N hydrogen bonding [N···N=2.725(4) Å; N–H···N=171.0(4)°] involving the protonated and non-protonated ends of the pyridyl urea moieties of the neighboring ionic species resulting in the formation of a 2D microporous network propagated approximately along *b*–*c* plane. The offset packing of such microporous 2D sheets effectively blocked the micropores in the crystal structures (Fig. 8).

It is interesting to note that except for **2c**, all the gelators found in this study are salts and therefore, the supramolecular

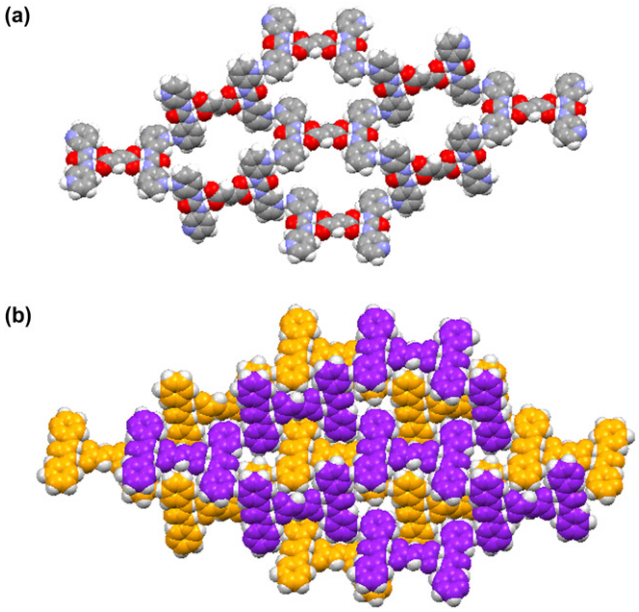

Figure 8. Crystal structure of **2g**: (a) self-assembly of 'I' shaped ionic species displaying 2D microporous architecture; (b) offset packing of 2D networks resulting into a non-microporous architecture.

structures in these compounds should logically be dictated by the urea-carboxylate synthon (Scheme 1). Indeed, the crystal structure of **1c** revealed the presence of the urea-carboxylate synthon, which further self-assembled into a microporous network (Fig. 2). On the other hand, hydrogelator **2c** whose urea counterpart is isomeric with that in **1c** is a complex rather than a salt and displayed pyridine-carboxylic acid synthon as expected (Scheme 1). Due to the *syn–anti* conformation of the urea derivative, the assembly of the ionic species resulted in an 1D helical network that further hydrogen bonded with the neighboring helical network producing microporous architecture (Fig. 4). The crystal structure of the hydrogelator salt **1d** also revealed the presence of the urea-carboxylate synthon, which further self-assembled into a microporous network (Fig. 3). It may be noted that the long 1D fiber morphology of the gel fibers (Fig. 1) can easily be formed from the preferential growth of the fiber crystals along the axis of propagation of the 1D zigzag chain in **1c**, microporous ladder-type primary supramolecular structure in **1d,** and the assembly of a few helical chains of ion pairs in **2c**.

The nongelator **2d** is a partial salt and its stoichiometry is 1:2 (acid/urea) unlike its hydrogelator counterpart **1d**. Thus, the urea-carboxylate synthon is formed at the carboxylate end of the adipic acid moiety in **2d**. Surprisingly, the carboxylic acid end displayed urea–carboxylic acid interactions via N–H···O hydrogen bonding instead of the pyridine-carboxylic acid synthon. The 'I' shaped ionic species, thus formed, further self-assembled into an 1D zigzag chain sustained by N–H···N hydrogen bonding involving protonated and non-protonated pyridine moieties of the interacting ionic species. Such chains are arranged into a planar array mediated by hydrogen bonding with solvate water molecules. Although, the crystal structure of **2d** does have some solvate water molecules included in the crystal lattice, the overall supramolecular network is not as microporous as it is in its hydrogelator counterpart **1d**.

Nongelators **1e** and **2e**, which are isomeric in their urea counterpart, are complete salt and partial salt, respectively. As a result, the pyridyl moieties of the urea derivatives **1** and **2** are fully protonated in **1e** and monoprotonated in **2e**, respectively. Thus, in **1e**, in addition to the urea-carboxylate synthon, the pyridinium–carboxylate interaction is also observed. Such interactions led to the formation of parallel arrays of 1D zigzag hydrogen bonded chains of ionic species. The micropores observed in this array do not occlude any solvate molecules in the crystal structure. On the other hand, monoanionic cyclobutane dicarboxylate synthon displayed the most frequently occurring carboxylic acid-carboxylate synthon in **2e** in addition to the urea-carboxylate synthon. As a result, a double toothed 2D zipper type of architecture is formed, which are efficiently zipped with the neighboring networks leaving no room for guest occlusion.

The most interesting structure among the nongelators is the structure of **2g** wherein the fumaric acid moiety is completely deprotonated by donating its protons to two urea derivatives. Thus, the carboxylate ends of the acid moiety hold two urea derivatives using the urea-carboxylate synthon. Such an 'I' shaped ionic species further hydrogen bonded with its neighbors using N–H···N hydrogen bonding involving protonated and non-protonated pyridyl moieties lead to the formation of a 2D hydrogen bonded network having large pores. However, no guest molecules have been found in the crystal structure. Instead, offset packing of such corrugated 2D sheets prevents the formation of effective microporous architecture.

3. Conclusion

A crystal engineering approach has been exploited to generate a series of new hydrogelators. Dicarboxylic acid composites of hydrogelator **1** and nonhydrogelator **2** led to the formation of a new class of hydrogelators. It is remarkable that four such composites of nongelator **2** turned out to be hydrogelators. All the hydrogelators, except **2c**, in the series are salts meaning that the supramolecular architectures in these salts are mainly governed by the urea-carboxylate synthon as also demonstrated by the crystal structure of **1c** and **1d**. On the other hand, **2c** is a hydrogen bonded complex displaying the pyridine-carboxylic acid synthon in its crystal structure. The ability to form a microporous architecture appears to be an important criterion for hydrogelation as demonstrated by the crystal structures of the gelators **1c**, **1d**, and **2c**. The fact that nongelator **2g** also displayed large pores within the primary supramolecular architecture perhaps indicates that microporosity in the crystalline solid state structure may be one of the important criterion but not a 'necessary and sufficient condition' for hydrogelation.

4. Experimental

4.1. Materials and physical measurements

Synthesis and characterization of *N*,*N*′-bis(4-pyridyl)urea **1** and *N*,*N*′-bis(3-pyridyl)urea **2** were previously reported by us.[11] All dicarboxylic acids (Aldrich) and the solvents used for gelation (A.R. grade, S.D. Fine Chemicals, India) were used without further purification. Microanalyses were

performed on a Perkin–Elmer elemental analyzer 2400, Series II. FTIR and ^{1}H NMR spectra were recorded using Perkin–Elmer Spectrum GX and 200 MHz Bruker Avance DPX_{200} spectrometers, respectively. Scanning electron microscopy (SEM) is performed on a LEO 1430VP. Powder X-ray diffraction patterns were recorded on XPERT Philips (Cu Kα radiation λ=1.5418 Å) diffractometer.

4.1.1. T_{gel} measurement. T_{gel} was measured by the following method. The gel was (1.0 ml) prepared in a test tube (15 mm diameter). A locally made glass ball weighing 0.195 g was placed on the gel surface. The test tube was then heated in an oil bath. The temperature (T_{gel}) was noted when the ball fell to the bottom of the test tube.

4.2. Synthesis

Salts are those where a complete proton transfer has taken from the acid to the amine. Adducts are those wherein complete proton transfer has not taken place; it can either be a partial salt (wherein the proton transfer is partial) or a molecular complex (wherein no proton transfer has taken place).

All the salts/adducts were synthesized by mixing corresponding acids with **1** and **2** in 1:1 molar ratio in MeOH at room temperature. In the case of salts/adducts of **1**, immediate precipitates were obtained except in the case of **1e**; whereas in the case of salts/adducts of **2**, immediate precipitates were not observed except in the case of **2a**. The reaction mixture was then evaporated at room temperature and the salts/adducts were isolated in near quantitative yields and used for further studies. In the cases of immediate precipitation, the precipitates were filtered, air dried, and used for gelation experiments and other studies. Due to the poor solubility of **1a**, ^{1}H NMR could not be recorded. X-ray powder diffraction patterns of the bulk solid and simulated patterns obtained from the corresponding single crystal X-ray data match reasonably well indicating uniformity of the crystalline morph as well as adduct formation in **2c**.

4.3. Analytical data

4.3.1. Oxalic acid–*N*,*N*′-bis(4-pyridyl)urea (1:1) salt (1a). Mp 210 °C. Anal. Calcd for $C_{13}H_{12}N_4O_5\cdot H_2O$: C, 48.45; H, 4.38; N, 17.38. Found: C, 48.7; H, 4.18; N, 17.78. FTIR (KBr, cm^{-1}): 3398, 3251, 3133, 3067, 2770, 2127, 1741, 1622, 1505, 1326, 1296, 1234, 1192, 1056, 906, 851, 831, 795, 750, 709, 608, 505.

4.3.2. Oxalic acid–*N*,*N*′-bis(3-pyridyl)urea (1:1) salt (2a). Mp 184–186 °C. Anal. Calcd for $C_{13}H_{12}N_4O_5\cdot H_2O$: C, 48.45; H, 4.38; N, 17.38. Found: C, 48.30; H, 4.18; N, 17.07. ^{1}H NMR (200 MHz, DMSO-d_6): δ=7.34–7.40 (2H, dd, J=4, 4 Hz, Py-H); 7.97–8.00 (2H, d, J=6 Hz, Py-H); 8.22–8.25 (2H, d, J=6 Hz, Py-H); 8.66–8.67 (2H, d, J=2 Hz); 9.23 (2H, s, N–H). FTIR (KBr, cm^{-1}): 3419, 3290, 3091, 2155, 1718, 1587, 1557, 1478, 1423, 1279, 1217, 1023, 953, 810, 766, 719, 678, 592, 503, 447.

4.3.3. Malonic acid–*N*,*N*′-bis(4-pyridyl)urea (1:2) salt (1b). Mp 170 °C. Anal. Calcd for $C_{25}H_{24}N_8O_6\cdot DMSO\cdot 1/2H_2O$: C, 52.33; H, 5.04; N, 18.08. Found: C, 52.45; H, 4.84; N, 17.83. ^{1}H NMR (200 MHz, D_2O): δ=3.24 (2H, s, –CH_2–); 7.99–8.02 (8H, d, J=6 Hz, Py-H); 8.53–8.56 (8H, d, J=6 Hz, Py-H). FTIR (KBr, cm^{-1}): 3410, 3264, 3134, 3046, 2669, 2363, 2139, 2034, 1739, 1665, 1622, 1557, 1512, 1459, 1410, 1352, 1329, 1305, 1235, 1192, 1100, 1053, 956, 835, 752, 691, 654, 584, 520, 499.

4.3.4. Malonic acid–*N*,*N*′-bis(3-pyridyl)urea (1:1) adduct (2b). Mp 160 °C. Anal. Calcd for $C_{14}H_{14}N_4O_5$: C, 52.83; H, 4.43; N, 17.60. Found: C, 52.44; H, 4.10; N, 17.76. ^{1}H NMR (200 MHz, D_2O): δ=3.36 (2H, s, –CH_2–); 7.67–7.74 (2H, m, Py-H); 8.15–8.18 (2H, d, J=6 Hz, Py-H); 8.32–8.35 (2H, d, J=6 Hz, Py-H); 8.82 (2H, s, Py-H). FTIR (KBr, cm^{-1}): 3359, 3212, 3071, 2997, 2170, 1918, 1720, 1642, 1596, 1563, 1481, 1403, 1364, 1331, 1314, 1291, 1259, 1230, 1130, 1055, 937, 916, 889, 842, 808, 745, 691, 663, 568, 489, 442.

4.3.5. Succinic acid–*N*,*N*′-bis(4-pyridyl)urea (1:2) salt (1c). Mp 194 °C. Anal. Calcd for $C_{26}H_{26}N_8O_6\cdot 2CH_3OH\cdot 3H_2O$: C, 50.60; H, 6.07; N, 16.86. Found: C, 50.78; H, 6.31; N, 16.01. ^{1}H NMR (200 MHz, DMSO-d_6): δ=2.43 (4H, s, –CH_2–CH_2–); 7.46–7.49 (8H, d, 6 Hz, Py-H); 8.38–8.42 (8H, d, 8 Hz, Py-H); 9.58 (br N–H). FTIR (KBr, cm^{-1}): 3443, 3137, 3035, 2979, 2944, 2538, 2159, 2027, 1942, 1736, 1658, 1627, 1542, 1508, 1479, 1404, 1385, 1331, 1298, 1231, 1197, 1137, 1051, 1029, 956, 881, 845, 762, 670, 626, 525, 501, 466.

4.3.6. Succinic acid–*N*,*N*′-bis(3-pyridyl)urea (1:1) complex (2c). Mp 178–180 °C. Anal. Calcd for $C_{15}H_{16}N_4O_5$: C, 54.21; H, 4.85; N, 16.86. Found: C, 54.15; H, 4.68; N, 16.50. ^{1}H NMR (200 MHz, MeOD): δ=2.56 (4H, s, –CH_2–CH_2–); 7.36–7.43 (2H, dd, J=5, 4.6 Hz, Py-H); 8.01–8.07 (2H, m, Py-H); 8.20–8.22 (2H, d, J=4 Hz, Py-H); 8.63 (2H, s, Py-H). FTIR (KBr, cm^{-1}): 3348, 3311, 3149, 3108, 2930, 2730, 2437, 1877, 1720, 1689, 1595, 1565, 1487, 1434, 1391, 1359, 1330, 1279, 1247, 1206, 1185, 1130, 1107, 1056, 997, 975, 945, 895, 844, 802, 766, 723, 701, 672, 558, 522, 411.

4.3.7. Adipic acid–*N*,*N*′-bis(4-pyridyl)urea (1:1) salt (1d). Mp 188 °C. Anal. Calcd for $C_{17}H_{20}N_4O_5$: C, 56.66; H, 5.59; N, 15.55. Found: C, 56.58; H, 5.13; N, 15.46. ^{1}H NMR (200 MHz, D_2O): δ=1.57 (4H, s, –CH_2–CH_2–); 2.24 (4H, s, –CH_2–COOH); 7.94–7.91 (4H, d, J=6.0 Hz, Py-H); 8.53–8.50 (4H, d, J=6.0 Hz, Py-H). FTIR (KBr, cm^{-1}): 3149, 2890, 1953, 1739, 1619, 1507, 1422, 1330, 1265, 1221, 1187, 1052, 1015, 939, 892, 841, 748, 705, 628, 522, 484.

4.3.8. Adipic acid–*N*,*N*′-bis(3-pyridyl)urea (1:1) adduct (2d). Mp 158–160 °C. Anal. Calcd for $C_{17}H_{20}N_4O_5$: C, 56.66; H, 5.59; N, 15.55. Found: C, 56.45; H, 5.57; N, 15.25. ^{1}H NMR (200 MHz, MeOD): δ=1.60–1.67 (4H, m, –CH_2–CH_2–); 2.26–2.33 (4H, t, J=4, 4 Hz, CH_2–COOH); 7.35–7.42 (2H, dd, J=4.8, 4.8 Hz, Py-H); 8.05–8.06 (2H, m, Py-H); 8.19–8.22 (2H, d, J=4.8, Py-H); 8.63–8.64 (2H, d, J=2 Hz, Py-H). FTIR (KBr, cm^{-1}): 3356, 3202, 3140, 3103, 2957, 2918, 2874, 2483, 1914, 1701, 1604, 1553, 1486, 1405, 1325, 1275, 1187, 1129, 1105, 1049, 1032, 908, 808, 706, 670, 658, 637, 539, 515, 491, 409.

4.3.9. 1,1-Cyclobutane dicarboxylic acid–*N*,*N*′-bis(4-pyridyl)urea (1:1) salt (1e). Mp 180 °C. Anal. Calcd for $C_{17}H_{18}N_4O_5$: C, 56.98; H, 5.06; N, 15.63. Found: C, 56.95; H, 4.85; N, 15.61. ^{1}H NMR (200 MHz, MeOD): δ=1.93–2.09 (2H, m, –CH_2–); 2.49–2.57 (4H, t, J=8, 8 Hz, –CH_2–COOH); 7.71–7.75 (4H, d, J =8 Hz, Py-H); 8.39–8.42 (4H, d, J =6 Hz, Py-H). FTIR (KBr, cm^{-1}): 3119, 3090, 2995, 2946, 1731, 1632, 1593, 1557, 1504, 1418, 1328, 1296, 1222, 1196, 1110, 1085, 1053, 972, 917, 864, 840, 754, 730, 690, 579, 517, 427.

4.3.10. 1,1-Cyclobutane dicarboxylic acid–*N*,*N*′-bis(3-pyridyl)urea (1:1) salt (2e). Mp 182 °C. Anal. Calcd for $C_{17}H_{18}N_4O_5$: C, 56.98; H, 5.06; N, 15.63. Found: C, 56.83; H, 4.96; N, 15.87. ^{1}H NMR (200 MHz, MeOD): δ=1.89–2.05 (2H, m, –CH_2–); 2.48–2.56 (4H, t, J=8, 8 Hz, –CH_2–COOH); 7.38–7.44 (2H, dd, J=4, 4 Hz, Py-H); 8.02–8.08 (2H, m, Py-H); 8.20–8.23 (2H, d, J=6 Hz, Py-H); 8.60–8.67 (2H, d, J=2 Hz, Py-H). FTIR (KBr, cm^{-1}): 3293, 3251, 3216, 3098, 3035, 2984, 2942, 2152, 1978, 1724, 1697, 1591, 1547, 1478, 1420, 1377, 1320, 1268, 1209, 1148, 1132, 1108, 1060, 1003, 933, 896, 799, 744, 700, 682, 630, 614, 528, 509, 439, 410.

4.3.11. Maleic acid–*N*,*N*′-bis(4-pyridyl)urea (1:1) salt (1f). Mp 184 °C. Anal. Calcd for $C_{15}H_{14}N_4O_5\cdot CH_3OH$: C, 53.04; H, 5.01; N, 15.46. Found: C, 52.50; H, 4.80; N, 14.99. ^{1}H NMR (200 MHz, DMF-d_7): δ=6.30 (2H, s, –CH=CH–); 7.86–7.89 (4H, d, J=6 Hz, Py-H); 8.53–8.57 (4H, d, J=8 Hz, Py-H). FTIR (KBr, cm^{-1}): 3420, 3269, 3132, 3031, 2946, 2824, 2661, 2362, 2077, 1964, 1740, 1617, 1505, 1364, 1318, 1290, 1219, 1192, 1105, 1053, 989, 893, 865, 832, 748, 661, 635, 584, 518, 435.

4.3.12. Maleic acid–*N*,*N*′-bis(3-pyridyl)urea (1:1) salt (2f). Mp 180 °C. Anal. Calcd for $C_{15}H_{14}N_4O_5$: C, 54.55; H, 4.27; N, 16.96. Found: C, 54.73; H, 4.19; N, 17.03. ^{1}H NMR (200 MHz, MeOD): δ=6.29 (2H, s, –CH=CH–); 7.52–7.59 (2H, dd, J=6, 6 Hz, Py-H); 8.11–8.17 (2H, m, Py-H); 8.28–8.30 (2H, d, J=4 Hz, Py-H); 8.83–8.84 (2H, d, J=2 Hz, Py-H). FTIR (KBr, cm^{-1}): 3625, 3350, 3312, 3149, 3109, 2929, 2435, 1889, 1720, 1613, 1594, 1565, 1486, 1434, 1404, 1391, 1359, 1330, 1279, 1247, 1207, 1185, 1130, 1106, 1055, 997, 975, 945, 895, 844, 802, 766, 701, 672, 612, 558, 522, 412.

4.3.13. Fumaric acid–*N*,*N*′-bis(4-pyridyl)urea (1:1) salt (1g). Mp 204 °C. Anal. Calcd for $C_{15}H_{14}N_4O_5$: C, 54.55; H, 4.27; N, 16.96. Found: C, 54.39; H, 3.91; N, 16.63. ^{1}H NMR (200 MHz, DMF-d_7): δ=6.67 (2H, s, –CH=CH–); 7.60–7.63 (4H, d, J=6 Hz, Py-H); 8.44–8.47 (4H, d, J=6 Hz, Py-H). FTIR (KBr, cm^{-1}): 3648, 3403, 3269, 3138, 3051, 2651, 2246, 2122, 2015, 1920, 1741, 1628, 1545, 1506, 1385, 1330, 1298, 1228, 1195, 1051, 1014, 959, 903, 876, 844, 796, 757, 674, 618, 583, 528, 502, 444.

4.3.14. Fumaric acid–*N*,*N*′-bis(3-pyridyl)urea (1:2) salt (2g). Mp 176 °C. Anal. Calcd for $C_{26}H_{24}N_8O_6\cdot 1.5H_2O$: C, 54.64; H, 4.76; N, 19.61. Found: C, 54.41; H, 4.26; N, 20.05. ^{1}H NMR (200 MHz, MeOD): δ=6.76 (2H, s, –CH=CH–); 7.38–7.44 (4H, dd, J=4, 4 Hz, Py-H); 8.02–8.07 (4H, m, Py-H); 8.20–8.23 (4H, d, J=6 Hz, Py-H); 8.66–8.67 (4H, d, J =2 Hz, Py-H). FTIR (KBr, cm^{-1}): 3092, 2920, 2361, 1715, 1633, 1600, 1563, 1482, 1387, 1326, 1243, 1223, 1190, 1063, 1026, 984, 902, 808, 746, 698, 672, 652, 627, 519.

4.3.15. L-Tartaric acid–*N*,*N*′-bis(4-pyridyl)urea (1:1) salt (1h). Mp 186 °C. Anal. Calcd for $C_{15}H_{16}N_4O_7$: C, 49.45; H, 4.43; N, 15.38. Found: C, 49.07; H, 4.31; N, 15.11. ^{1}H NMR (200 MHz, D_2O): δ=4.41 (2H, s, –CH–OH); 8.02–8.05 (4H, d, J=6 Hz, Py-H); 8.53–8.56 (4H, d, J=6 Hz, Py-H). FTIR (KBr, cm^{-1}): 3396, 3135, 3049, 2678, 2144, 2033, 1740, 1665, 1621, 1558, 1500, 1512, 1302, 1234, 1197, 1099, 1052, 956, 836, 752, 687, 655, 584, 520, 497.

4.3.16. L-Tartaric acid–*N*,*N*′-bis(3-pyridyl)urea (1:1) salt (2h). Mp 172 °C. Anal. Calcd for $C_{15}H_{16}N_4O_7\cdot 3H_2O$: C, 43.06; H, 5.30; N, 13.39. Found: C, 42.97; H, 5.18; N, 13.38. ^{1}H NMR (200 MHz, MeOD): δ=4.55 (2H, s, –CH–OH); 7.37–7.43 (2H, dd, J=5.2, 4 Hz, Py-H); 8.03–8.08 (2H, m, Py-H), 8.21–8.23 (2H, d, 4 Hz, Py-H), 8.69 (2H, s, Py-H). FTIR (KBr, cm^{-1}): 3430, 3308, 3078, 2922, 2823, 1716, 1648, 1549, 1473, 1411, 1360, 1311, 1233, 1123, 1080, 984, 921, 890, 811, 789, 750, 682, 602, 522.

4.4. Single crystal X-ray diffraction

X-ray quality crystals of **1e**, **1d**, **1c**, and **2e** were obtained by the slow evaporation of water/MeOH mixture at room temperature. Crystals of **2c** and **2g** were obtained from MeOH, while that of **2d** was obtained from water.

X-ray single crystal data were collected using Mo Kα (λ=0.7107 Å) radiation on a SMART APEX diffractometer equipped with CCD area detector. Data collection, data reduction, and structure solution/refinement were carried out using the software package of SMART APEX. All structures were solved by direct methods and refined in a routine manner. In all cases, non-hydrogen atoms were treated anisotropically. Whenever possible, the hydrogen atoms were located on a difference Fourier map and refined. In other cases, the hydrogen atoms were geometrically fixed at their idealized positions.

Crystallographic data for the structural analysis of compounds reported herein have been deposited at the Cambridge Crystallographic Data Center, CCDC nos. 619057–619063. Copies of this information may be obtained free of charge from The Director, CCDC, 12 Union Road, Cambridge, CB2 1EZ, UK (fax: +44 1233 336 033; e-mail: deposit@ccdc.cam.ac.uk or http://www.ccdc.cam.ac.uk).

Acknowledgements

Ministry of Environment and Forests, New Delhi, India, is thankfully acknowledged for financial support. D.K.K. thanks CSIR for a SRF fellowship.

Supplementary data

Supplementary data associated with this article can be found in the online version, at doi:10.1016/j.tet.2007.02.005.

References and notes

1. For reviews on LMOGs: (a) Sangeetha, N. M.; Maitra, U. *Chem. Soc. Rev.* **2005**, *34*, 821–836; (b) Estroff, L. A.; Hamilton, A. D. *Chem. Rev.* **2004**, *104*, 1201–1218; (c) van Esch, J. H.; Feringa, B. L. *Angew. Chem., Int. Ed.* **2000**, *39*, 2263–2266; (d) Abdallah, D. J.; Weiss, R. G. *Adv. Mater.* **2000**, *12*, 1237–1247; (e) Terech, P.; Weiss, R. G. *Chem. Rev.* **1997**, *97*, 3133–3160; For recent studies on LMOGs: (f) Shirakawa, M.; Fujita, N.; Shinkai, S. *J. Am. Chem. Soc.* **2005**, *127*, 4164–4165; (g) Hirst, A. R.; Smith, D. K.; Harrington, J. P. *Chem.—Eur. J.* **2005**, *11*, 6552–6559; (h) van Bommel, K. J. C.; van der Pol, C.; Muizebelt, I.; Friggeri, A.; Heeres, A.; Meetsma, A.; Feringa, B. L.; van Esch, J. *Angew. Chem., Int. Ed.* **2004**, *43*, 1663–1667; (i) Čaplar, V.; Žinić, M.; Pozzo, J.-L.; Fages, F.; Mieden-Gundert, G.; Vögtle, F. *Eur. J. Org. Chem.* **2004**, 4048–4059; (j) Maji, S. K.; Malik, S.; Drew, M. G. B.; Nandi, A. K.; Banerjee, A. *Tetrahedron Lett.* **2003**, *44*, 4103–4107; (k) John, G.; Zhu, G.; Li, J.; Dordick, J. S. *Angew. Chem., Int. Ed.* **2006**, *45*, 4772–4775; (l) Yang, Z.; Liang, G.; Xu, B. *Chem. Commun.* **2006**, 738–740.
2. (a) Ilmain, F.; Tanaka, T.; Kokufuta, E. *Nature* **1991**, *349*, 400–401; (b) Holtz, J. H.; Asher, S. A. *Nature* **1997**, *389*, 829–832; (c) Simonsen, L.; Hovgaard, L.; Mortensen, P. B.; Brondsted, H. *Eur. J. Pharm. Sci.* **1995**, *3*, 329–337; (d) Osada, Y.; Gong, J. P. *Adv. Mater.* **1998**, *10*, 827–837; (e) Weissman, J. M.; Sunkara, H. B.; Tse, A. S.; Asher, S. A. *Science* **1996**, *274*, 959–960; (f) Andrianov, A. K.; Cohen, S.; Visscher, K. B.; Payne, L. G.; Allcock, H. R.; Langer, R. *J. Controlled Release* **1993**, *27*, 69–77; (g) *Polymer Gels and Networks*; Osada, Y., Khokhlov, A. R., Eds.; Marcel Dekker: New York, NY, 2002; (h) Chu, Y. H.; Chen, J. K.; Whitesides, G. M. *Anal. Chem.* **1993**, *65*, 1314–1322; (i) Lee, K.; Asher, S. A. *J. Am. Chem. Soc.* **2000**, *122*, 9534–9537; (j) Tiller, J. C. *Angew. Chem., Int. Ed.* **2003**, *42*, 3072–3075.
3. (a) Kavanagh, G. M.; Ross-Murphy, S. B. *Prog. Polym. Sci.* **1998**, *23*, 533–562; (b) Perka, C.; Spitzer, R. S.; Lindenhayn, K.; Sittinger, M.; Schultz, O. J. *Biomed. Mater. Res.* **2000**, *49*, 305–311; (c) Chenite, A.; Chaput, C.; Wang, D.; Combes, C.; Buschmann, M. D.; Hoemann, C. D.; Leroux, J. C.; Atkinson, B. L.; Binette, F.; Selmani, A. *Biomaterials* **2000**, *21*, 2155–2161.
4. Peppas, N. A.; Bures, P.; Leobandung, W.; Ichikawa, H. *Eur. J. Pharm. Biopharm.* **2000**, *50*, 27–46.
5. Ostuni, E.; Kamaras, P.; Weiss, R. G. *Angew. Chem., Int. Ed.* **1996**, *35*, 1324–1326.
6. (a) Ballabh, A.; Trivedi, D. R.; Dastidar, P. *Chem. Mater.* **2003**, *15*, 2136–2140; (b) Trivedi, D. R.; Ballabh, A.; Dastidar, P.; Ganguli, B. *Chem.—Eur. J.* **2004**, *10*, 5311–5322; (c) Trivedi, D. R.; Ballabh, A.; Dastidar, P. *J. Mater. Chem.* **2005**, *15*, 2606–2614.
7. (a) Desiraju, G. R. *Crystal Engineering: The Design of Organic Solids*; Elsevier: Amsterdam, 1989; (b) Desiraju, G. R. *Angew. Chem., Int. Ed. Engl.* **1995**, *34*, 2311–2327.
8. (a) Trivedi, D. R.; Ballabh, A.; Dastidar, P. *Cryst. Growth Des.* **2006**, *6*, 763–768; (b) Trivedi, D. R.; Dastidar, P. *Chem. Mater.* **2006**, *18*, 1470–1478; (c) Ballabh, A.; Trivedi, D. R.; Dastidar, P. *Org. Lett.* **2006**, *8*, 1271–1274; (d) Trivedi, D. R.; Dastidar, P. *Cryst. Growth Des.* **2006**, *6*, 1022–1026; (e) Ballabh, A.; Trivedi, D. R.; Dastidar, P. *Chem. Mater.* **2006**, *18*, 3795–3800.
9. (a) Kumar, D. K.; Jose, D. A.; Dastidar, P.; Das, A. *Chem. Mater.* **2004**, *16*, 2332–2335; (b) Kumar, D. K.; Jose, D. A.; Dastidar, P.; Das, A. *Langmuir* **2004**, *20*, 10413–10418.
10. A recent report suggests that such correlation between microporosity and gel formation may also be true for some organogel system. Lebel, O.; Perron, M.-E.; Maris, T.; Zalzal, S. F.; Nanci, A.; Wuest, J. D. *Chem. Mater.* **2006**, *18*, 3616–3626.
11. Kumar, D. K.; Jose, D. A.; Das, A.; Dastidar, P. *Chem. Commun.* **2005**, 4059–4061.
12. While this manuscript was under preparation, the structure of **2c** was reported in a different context: Reddy, L. S.; Basavoju, S.; Vangala, V. R.; Nangia, A. *Cryst. Growth Des.* **2006**, *6*, 161–173.